

# Fluorescent Bacteria Encapsulated in Sol–Gel Derived Silicate Films

J. Rajan Premkumar, Eran Sagi, Rachel Rozen, Shimshon Belkin,  
Alexander D. Modestov, and Ovadia Lev\*

Division of Environmental Sciences, The Fredy and Nadine Herrmann Graduate School of Applied Science, The Hebrew University of Jerusalem, Jerusalem 91904, Israel

Received January 14, 2002. Revised Manuscript Received April 9, 2002

Recombinant fluorescent *E. coli* cells were encapsulated in sol–gel derived silicate films. Green and red fluorescent proteins expression by recombinant *E. coli* strains within the silicate film were studied. The effect of the preparation protocol on the viability of the encapsulated cells and their ability to express the fluorescent proteins in response to genotoxicity stress were evaluated. Confocal microscopy studies revealed a homogeneous distribution of the recombinant cells within the silicate film. We further showed by confocal microscopy studies that the encapsulated cells do not divide within the silicate film. Further, dynamic green fluorescent protein expression studies of a single encapsulated cell were carried out for the first time. No contamination of the surroundings by the encapsulated cells or contamination of the encapsulated culture by the surrounding population of bacteria was observed. The implications of these observations for dual sensing and multistep biosynthesis and biodegradation are discussed.

## Introduction

Whole cell–silicate hybrids are an emerging class of materials that combine the physical properties and the biocompatibility of inorganic silicates with the ability of cells to respond to environmental stimuli and influence their environment. Such hybrids entail great promise for intelligent biocatalysis and *in vivo* bioregulated catalysis, as well as for the somewhat less ambitious ecodiagnostics and early warning toxicity sensing. The emergence of this class of composites is a natural step in the evolution of sol–gel hybrids. Sol–gel science is gradually evolving from a technology for synthesis of pure inorganic materials to a field that deals with inorganic–organic hybrids in general and excels particularly in biochemical–inorganic composites. This evolution is accompanied by increased complexity—reaching ultimate intricacy with the successful encapsulation of intact cells.<sup>1–4</sup> The functionality of the emerging class of live cell–ceramic hybrids is largely dependent on the way the encapsulating hosts influence the cells' physiology, which arouses new challenges pertaining to the inorganic matrix effects and the way that it alters cell physiology, productivity, and proliferation. This manuscript is aimed at employing methods that may help in resolving questions related to the well being of the cells in the silicate matrixes and in resolving the distribution of live cells in silicate gels. By using

these methods, we illuminate specific properties of the encapsulated hybrids that distinguish them from the native cultures.

Despite the undisputed importance and technical challenges involved, there are only a few reports on the encapsulation of live cells in sol–gel matrixes.<sup>5–17</sup> Carturan and co-workers reported the immobilization of *Saccharomyces cerevisiae* yeasts and *Coronilla vaginalis* plant cells in silicate matrixes.<sup>6</sup> Carturan and co-

(5) (a) Branyik, T.; Kuncova, G.; Paca, J.; Demnerova, K. *J. Sol–Gel Sci. Technol.* **1998**, *13*, 283. (b) Livage, J.; Coradin, T.; Roux, C. *J. Phys.: Condens. Mater.* **2001**, *13*, R673. (c) Coiffier, A.; Coradin, T.; Roux, C.; Bouvet, O. M. M.; Livage, J. *J. Mater. Chem.* **2001**, *11*, 2039. (d) Finnie, K. S.; Bartlett, J. R.; Woolfrey, J. L. *J. Mater. Chem.* **2000**, *10*, 1099. (e) Kawakami, K.; Furukawa, S. Y. *Appl. Biochem. Biotechnol.* **1997**, *67*, 23. (f) Armon, R.; Dosoretz, C.; Starosvetsky, J.; Orshansky, F.; Saad, I. *J. Biotechnol.* **1996**, *51*, 279.

(6) (a) Carturan, G.; Camponstrini, R.; Dire, S.; Scardi, V.; De Alteris, E. *J. Mol. Catal.* **1989**, *57*, L13. (b) Camponstrini, R.; Carturan, G.; Caniato, R.; Piovan, A.; Filippini, R.; Innocenti, G.; Cappelletti, E. M. *J. Sol–Gel Sci. Technol.* **1996**, *7*, 87.

(7) Muraca, M.; Vileia, M. T.; Zanussoa, E.; Ferrareissa, C.; Granatoa, A.; Doninsegna, S.; Dal Monteb, R.; Carraroc, P.; Carturan, G. *Transplant. Proc.* **2000**, *32*, 2713.

(8) Peterson, K. P.; Peterson, C. M.; Pope, E. J. A. *Proc. Soc. Exp. Biol. Med.* **1998**, *218*, 365.

(9) Bressler, E.; Braun, S. *J. Sol–Gel Sci. Technol.* **1996**, *7*, 129.

(10) Bressler, E.; Braun, S. *J. Chem. Technol. Biotechnol.* **2000**, *75*, 66.

(11) Bergogne, L.; Fennouh, S.; Guyon, S.; Livage, J.; Roux, C. *Mol. Cryst. Liq. Cryst.* **2000**, *354*, 667.

(12) Chia, S. Y.; Urano, J.; Tamanoi, F.; Dunn, B.; Zink, J. I. *J. Am. Chem. Soc.* **2000**, *122*, 6488.

(13) Fennouh, S.; Guyon, S.; Jourdat, C.; Livage, J.; Roux, C. *Acad. Sci. Paris Iic.* **1999**, *2*, 625.

(14) Fennouh, S.; Guyon, S.; Livage, J.; Roux, C. *J. Sol–Gel Sci. Technol.* **2000**, *19*, 647.

(15) Premkumar, J.; Lev, O.; Marks, R. S.; Polyak, B.; Rosen, R.; Belkin, S. *Talanta* **2001**, *55*, 1029.

(16) Premkumar, J.; Lev, O.; Rosen, R.; Belkin, S. *Adv. Mater.* **2001**, *13*, 1773.

(17) Premkumar, J.; Lev, O.; Rosen, R.; Belkin, S. *Anal. Chim. Acta*, in press.

\* To whom correspondence should be addressed.

(1) Braun, S.; Rappoport, S.; Zusman, R.; Avnir, D.; Ottolenghi, M. *Mater. Lett.* **1990**, *10*, 1.

(2) Avnir, D. *Acc. Chem. Res.* **1995**, *28*, 328.

(3) Avnir, D.; Braun, S.; Lev, O.; Ottolenghi, M. *Chem. Mater.* **1994**, *6*, 1605.

(4) Dave, C.; Dunn, B.; Valentine, J. S.; Zink, J. I. *Anal. Chem.* **1994**, *66*, 1120.

**Table 1. Bioluminescent and Fluorescent Bacterial Strains and the Inducers Used in the Present Study**

strain designation	promotor/sensitivity	detection mode	inducer used in this study	wavelength (nm)			ref
				excitation	emission		
TV1061	grpE/general stress	luminescence	ethanol	2% (v)		495	20
ES2R (GFP)	recA/genotoxicity	fluorescence	MMC	1.2 $\mu$ M	395	510	
RS2R(RFP)	recA/genotoxicity	fluorescence	NA	0.25 mM	558	583	

workers further showed viability of rat hepatocytes in layered  $\text{SiO}_2$ -collagen matrixes,<sup>7</sup> and Pope and co-workers<sup>8</sup> encapsulated pancreatic cells in sol-gel silicates. Braun used silica-alginate encapsulation for studies of the biosynthetic pathway of itaconic acid in fungus *Aspergillus terreus*.<sup>9,10</sup> Livage and Roux studied the encapsulation of *Leishmania* parasites for recognition of antibodies in human blood.<sup>11</sup> Zink, Dunn, and co-workers patterned silicate networks with bacterial cells.<sup>12</sup>

Sol-gel encapsulation of *Escherichia coli* was studied extensively by Livage and co-workers.<sup>13,14</sup> Recently, we demonstrated the attachment or encapsulation of genetically engineered luminous *E. coli* cells on or within silicate films.<sup>15,16</sup> The hybrid was used for monitoring of externally induced physiological stress,<sup>17</sup> for ecosensing, and for reporting the stress induced by the silicate cages under different sol-gel encapsulation procedures.<sup>16</sup>

In this article we use a combination of two emerging tools in order to gain deeper insight on the viability, activity, and distribution of the encapsulated cells in silicate matrixes. First, we use genetically engineered bacteria capable of expressing green and red fluorescent proteins (GFP and RFP) which serve in this research as biomarkers for cell activity and reporters for the cell distribution in the silicate network. Additionally, we use confocal microscopy in order to trace the spatiotemporal distribution of the fluorescent cells within sol-gel films.

Genetically engineered microbial reporter strains, such as those used in this study, couple a gene promotor as a sensing element for chemical or physical change to a reporter gene(s) coding for measurable protein(s). The promotor senses the presence of a target molecule(s) and activates transcription of the reporter gene. Subsequent translation of the reporter mRNA produces a protein that generates a detectable signal.<sup>18</sup> Different reporter proteins are used in recombinant biosensing systems, allowing luminometric, fluorimetric, electrochemical, or colorimetric detection. The fluorescent proteins GFP and RFP used in the present study are highly stable, are readily detectable, and do not require a substrate (except for oxygen) or a cofactor for their synthesis.<sup>19a</sup> We have fused the structural genes of these proteins (*gfp* and *DsRed*, respectively) to the promoter of the *recA* gene of *Escherichia coli* and introduced it into the same bacterium. Bacterial constructs harboring *recA*::reporter fusions were previously shown<sup>19</sup> to be sensitive sensors of genotoxins (mutagens etc.).

(18) Kohler, S.; Belkin, S.; Schmid, R. D. *Fres. J. Anal. Chem.* **2000**, 366, 769.

(19) (a) Daunert, S.; Barrett, G.; Feliciano, J. S.; Shetty, R. S.; Shrestha, S.; Smith-Spencer, W. *Chem. Rev.* **2000**, 100, 2705. (b) Kostynska, M.; Leung, K. T.; Lee, H.; Trevors, J. T. J. *Microbiol. Methods* **2002**, 48, 43. (c) Vollmer, A. C.; Belkin, S.; Smulski, D. R.; Van Dyk, T. K.; LaRossa, R. A. *Appl. Environ. Microbiol.* **1997**, 63, 2566. (d) Davidov, Y.; Rosen, R.; Smulski, D. R.; Van Dyk, T. K.; Vollmer, A. C.; Elsemore, D. A.; LaRossa, R. A.; Belkin, S. *Mutat. Res.* **2000**, 466, 97.

Laser scanning confocal microscopy provides the ability to localize the field of illumination and detection by small apertures, which facilitates virtual sectioning of the thick film specimen containing the fluorescent cells. By this method it is possible to obtain diffraction-limited resolution—usually a couple of hundred nanometers—which is well below the size of a single *E. coli* cell (a cylindrical rod of ca. 1  $\mu\text{m} \times 2 \mu\text{m}$ ).

Accordingly, the article starts with a description of the specific details of the encapsulation procedure, which shows how bulk fluorescence depends on preparation conditions. Then we address the spatial bioactivity distribution within the silicate gel using a combination of engineered fluorescent bacteria and confocal microscopy. Finally, we present the time course of single cell induction and fluorescence within the silicate matrix. As far as we know, none was presented before.

## Experimental Section

**Materials.** Tetramethylorthosilane (TMOS), nalidixic acid (NA), and mitomycin C (MMC) were purchased from Aldrich (WI).

The bacterial strains (and the inducers used in this study) are listed in Table 1. Two of them (ES2R and RS2R) harbor a multicopy plasmid containing a fusion of the *recA* promoter to either GFP or RFP genes, respectively. A detailed description of their construction will be published elsewhere. The third strain (TV1061)<sup>20</sup> is a bioluminescent “general toxicity” sensor, included as a control species in one of the experiments. All three constructs are based on *E. coli* RFM443.<sup>20</sup>

Prior to encapsulation, the bacterial strains were grown overnight in Luria-Bertani (LB) broth<sup>21</sup> containing 100  $\mu\text{g}/\text{mL}$  ampicillin to ensure plasmid maintenance. The culture was continuously shaken at 37 °C, and growth was monitored using a Klett-Summerson colorimeter (Monostat corporation). The culture was diluted with fresh LB medium and then regrown under the same conditions to an early exponential growth phase (20 Klett units, corresponding to about 10<sup>8</sup> cells/mL, as previously described).<sup>20,22</sup>

For the measurement of the effect of mitomycin C (MMC) or nalidixic acid (NA) on the luminescence response of suspended bacteria, early exponential growth cultures were exposed to the inducers, and then a sample was mixed with an equal amount of LB medium. One hundred microliters of the mixture were placed in duplicate wells of an opaque white microtiter plate (Costar Europe, Bdhoevedrop, The Netherlands). The microtiter plates were incubated in a temperature-controlled (26 °C) incubator, and fluorescence was periodically measured with a microtiter plate fluorescence/luminescence meter (Victor2, EG&G Wallac 1420, Turku, Finland). Fluorescence and luminescence values are presented in the instrument's arbitrary relative units (RFU or RLU, respectively). LB medium and 1:1 medium/culture mixtures without the inducer served as controls. The luminescence and fluorescence

(20) Van Dyk, T. K.; Majarian, W. R.; Konstantinov, K. B.; Young, R. M.; Dhurjati, P. S.; La Rossa, R. A. *Appl. Environ. Microbiol.* **1994**, 60, 1414.

(21) Miller, J. H. *Experiments in Molecular Genetics*; Cold Spring Harbor Laboratory Press: Spring Harbor, NY, 1972.

(22) Belkin, S.; Smulski, D. R.; Dadon, S.; Vollmer, A. C.; Van Dyk, T. K.; La Rossa, R. A. *Water Res.* **1997**, 31, 3009.

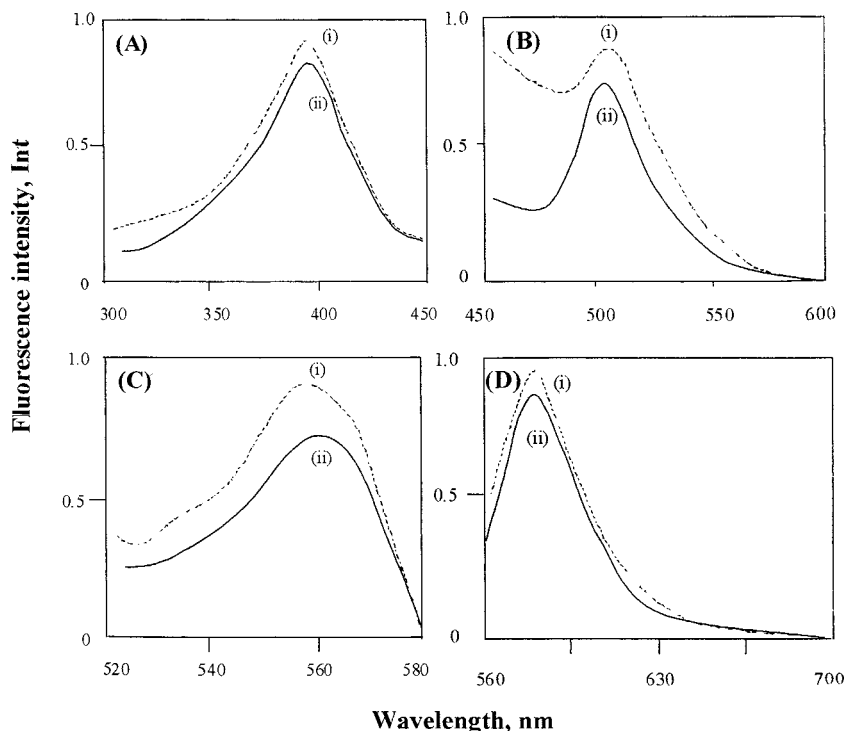


**Figure 1.** (A) Excitation and (B) emission spectra of (i) ES2R (GFP producing cells) suspension and (ii) ES2R in sol-gel silicate, and (C) excitation and (D) emission spectra of (i) RS2R (RFP producing cells) suspension and (ii) RS2R in sol-gel silicate.

responses of the encapsulated bacteria were measured by a similar procedure, with the bacteria encapsulated substrate placed in a 100  $\mu$ L solution of LB medium and inducer in duplicate microtiter wells.

Emission and excitation fluorescence spectra were obtained with a Perkin-Elmer luminescence spectrometer LS 50 B (U.K.). Confocal microscopy studies were conducted with a Bio-Rad MRC 600 (USA) confocal microscope equipped with an argon laser. Detection of the green and red fluorescence proteins was conducted with 395 and 558 nm wavelength band-pass filters for GFP and RFP, respectively.

**Preparation of Bacteria-Loaded Thick Silicate Films.** Glass slides (1 mm thickness) were purchased from Paul Marienfld GmbH & Co. KG Laboratory Glassware Company (Germany) and cut to  $4 \times 4$  mm<sup>2</sup> pieces. The glass slides were cleaned successively with a 1:1:1 acetone/ethanol/chloroform mixture, soap solution, piranha (H<sub>2</sub>SO<sub>4</sub>/H<sub>2</sub>O<sub>2</sub>, 4:1) solution, distilled water, and 1 M NaOH. Then, the clean glass pieces were dried for 1 h in an 80 °C oven.

The sol-gel mixtures were prepared by mixing 4 mL of tetramethylorthosilane (TMOS, Aldrich, WI) with 2 mL of distilled water and 0.5 mL of 0.1 M HCl. The mixture was sonicated for 10 min to ensure uniformity and left to age at 4 °C for 1 day. Three milliliters of the *E. coli* suspension (20 Klett units, 10<sup>8</sup> cells/mL) in LB medium were thoroughly mixed with 0.5 mL of the sol-gel solution, and 0.01 mL which contained approximately 10<sup>6</sup> cells of the mixture was then coated on the glass plate and dried for 5 min under ambient conditions (ca. 20 °C). The *E. coli*-sol-gel films were washed with phosphate buffer and then with LB medium, both at pH 7, and kept in microtiter plate wells in phosphate buffer. For the quantification of the effect of pH, we have corrected the pH of the LB broth to the specified level and then mixed it with 4 mL of tetramethoxysilane and 2 mL of distilled water (without addition of hydrochloric acid). Thus, the initial pH of the mixture is essentially identical to the pH of the LB broth. All the bulk fluorescence tests were conducted in duplicates. The relative difference between all the duplicates reported here was less than 10% of their average.

**Luria-Bertani (LB) Broth.** The LB broth cultivation medium contained 5 g/L NaCl, 5 g/L yeast extract, and 10 g/L

tryptone.<sup>21</sup> Ampicillin (100  $\mu$ g/mL) was added to the LB broth to ensure plasmid maintenance.

## Results and Discussion

**GFP and RFP Expression by Recombinant *E. coli* Strains within the Silicate Film.** The first part of this study was devoted to the encapsulation of the fluorescent *E. coli* strains in thick silicate films. We compared the responses of the encapsulated cells to those of suspended cells under the same constraints and elucidated optimized preparation parameters for maintaining the viability of the cells during the encapsulation procedure.

The model fluorescent organisms that were selected for this study contained fusion of the promoter of the *recA* gene to either the GFP (strain ES2R) or the RFP (strain RS2R) genes. Mitomycin C (MMC) was used to induce the ES2R cells, and nalidixic acid (NA) was used to induce the RS2R cells.

**Fluorescence Spectra.** Parts A and B of Figure 1 show the emission and excitation spectra of encapsulated ES2R and RS2R cells (a) and suspensions. We used 395 and 510 nm wavelengths for excitation and emission studies of the GFP encoding cells and 558 and 583 nm for the RFP encoding cells. The ES2R and RS2R cells were induced by immersion in 1.2  $\mu$ M MMC or 0.25 mM NA in LB medium for 17 h prior to the fluorescence measurements. The emission and excitation spectra were practically unaffected by the presence of the silicate cages; that is, we obtain 510 and 583 nm emission peaks and 395 and 558 nm excitation peaks for GFP and RFP, respectively. These values are also identical to previously reported values for the fluorescence of intracellular GFP and RFP.<sup>19</sup> This is not entirely surprising. The green and red fluorescent

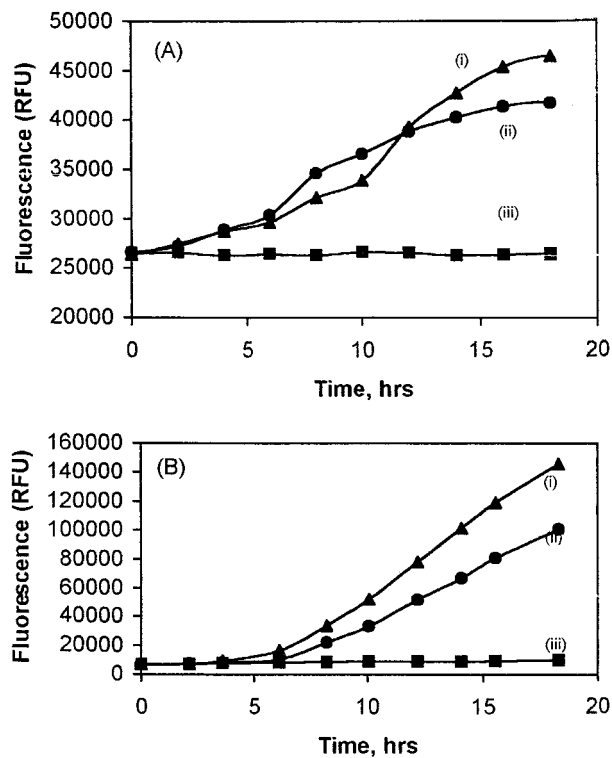


**Figure 2.** (A) Time course of the fluorescence intensity of ES2R cells ( $10^6$  cells): (i) ES2R suspension in MMC (1.2  $\mu$ M); (ii) ES2R encapsulated sol-gel silicate in MMC (1.2  $\mu$ M); (iii) ES2R suspension in LB medium without added inducer. (B) Time course of the fluorescence intensity of RS2R cells ( $10^6$  cells): (i) RS2R suspension in NA (0.25 mM); (ii) RS2R encapsulated sol-gel silicate in NA (0.25 mM); (iii) RS2R suspension in LB medium without added inducer.

proteins are intracellular proteins, which do not come in direct contact with the silicate shell, and thus the fluorescence response is unaffected by the presence of the silicate. The lower light scattering that is observed for the free cultures may have practical implications on the minimal detection limit and the signal/noise level of sensing elements based on encapsulated cells.

**Fluorescence Induction Time Course.** Figure 2 depicts the time course of fluorescence evolution of the ES2R and RS2R *E. coli*–silicate coated glass slides after exposure to 1.2  $\mu$ M MMC and 0.25 mM NA, respectively. Excitation and emission wavelengths were 395 and 510 nm for the GFP and 558 and 583 nm for RFP, respectively. The optical responses are presented in arbitrary intensity units as read by the Victor<sup>2</sup> fluorometer. For comparison, the responses of a nonimmobilized cell suspension containing the same number of bacteria,  $10^6$  cells per microtiter well, are presented on the same figure. The responses of control *E. coli* suspensions that have undergone identical treatment but without exposure to the inducers are also depicted as the lower line on each frame in Figure 2. The responses of encapsulated *E. coli* subjected to the same conditions but without the inducer were identical to curve iii and therefore were not shown. We present here only the response of ES2R *E. coli* to MMC and the response of RS2R to NA, though the response of ES2R to NA and the response of RS2R to MMC followed very similar patterns. The specific responses of the encapsulated and free cells are very similar for both ES2R and RS2R cells. The somewhat lower response of the encapsulated *E.*

*coli* cells can be attributed to one of the following reasons: (1) partial inactivation of the cells during the encapsulation procedure or (2) a much lower proliferation rate of the cells. We tend to attribute the lower response to a combination of the two reasons and support our hypothesis by the confocal microscope studies that are depicted below.

The increase in fluorescence intensity measured over the 15 h of the experiments was not caused by bacterial growth, as evidenced by the fact that a much smaller fluorescence increase was observed for the control cells exposed to the same conditions (lower curves in Figure 2A and B). A clearer and unequivocal support for this interim conclusion is given below by the confocal microscope studies. Thorough rinsing of the cell–silicate hybrids caused less than a 5% decrease in fluorescence (not shown), suggesting that the cells were indeed solidly embedded in the sol–gel matrix. For the same reason, there was no residual fluorescence in the medium after removal of the *E. coli* encapsulated glass plates from the microtiter wells, indicating that the fluorescence was generated by the caged bacteria and not by leached cells.

It should be mentioned that from a diagnostics point of view, which is not the center of this article, three practical drawbacks of the recombinant GFP- and RFP-producing *E. coli* for sensing applications can be noted: (1) The response time is too slow for early warning detectors. Unlike the induction of luminescence,<sup>15,16</sup> which takes some 30–120 min, the synthesis of the fluorescent proteins occurs on a much larger time scale of 2–20 h. This time lag is not caused by a mass transport barrier, since the time response of the suspended bacteria is as long and follows a similar pattern. (2) GFP and RFP are relatively stable, and thus the response is cumulative rather than differential, which makes a potential fluorescence sensor less sensitive. This attribute is also responsible for the next drawback. (3) The background fluorescence of the GFP- and RFP-producing cultures is rather high for the encapsulated as well as for the free bacteria. To a certain degree, the background can be lowered by the choice of less active promoters; however, a large 585 background fluorescence prevails even in the LB medium.

**Fluorescence Intensity and Its Dependence on the Concentrations of the Inducers and Sol-Gel Preparation Protocols.** The dependence of the expression of RFP and GFP in response to genotoxicity induction by different levels of NA and MMC inducers, respectively, is depicted in Figure 3. All tests were conducted in a similar manner. Films containing  $10^6$  ES2R or RS2R cells were exposed to LB medium containing different levels of the respective inducers for 17 h, followed by fluorescence intensity measurements (for the emission and excitation wavelengths depicted above). Parts A and B of Figure 3 show a clear dose-response curve which levels off or even exhibits a decrease for high inducer concentrations. The decrease is attributed to cell damage or death due to toxic substance doses. Similar curves were obtained for other exposure durations. The response curves of nonimmobilized cultures of the same bacteria were very similar.

Figure 4 depicts the dependence of the capability of the encapsulated bacteria to express fluorescent pro-

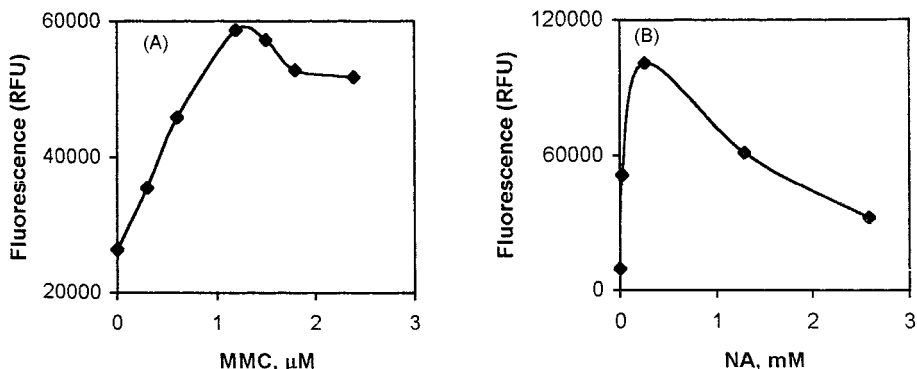


**Figure 3.** Concentration-fluorescence curves of recombinant *E. coli*: (A) ES2R encapsulated sol-gel silicate exposed to the specified concentrations of MMC; (B) RS2R encapsulated sol-gel silicate exposed to the specified NA concentrations. Incubation time, 17 h;  $10^6$  cells were used for each test.

teins on several characteristic features of the encapsulation procedure. All tests were conducted in a similar manner. The films were prepared as depicted in the basic preparation conditions (described in the Experimental Section) except for one preparation variable that was altered systematically, and then the bacteria were stored overnight at 4 °C. After this time, the encapsulated cells were exposed to the respective inducers for 17 h, and then the fluorescence response was measured.

Figure 4A demonstrates the dependence of the fluorescence of ES2R and RS2R-silicate matrixes on the initial pH of the LB medium used to produce the hybrid plates. We prefer to specify the pH of the LB medium rather than the pH of the resultant organic mixture because the latter is not well defined. Figure 4A shows that optimal preparation conditions were around pH 7.5 with residual viability throughout the pH range 5–9, in accordance with the behavior of native *E. coli*.<sup>23</sup>

We used pH 7 for the preparation of the cell-silicate hybrids with varying water-to-silicon ratio, *r* (*r* represents the molar H<sub>2</sub>O/Si ratio in the sol-gel precursors, including the H<sub>2</sub>O that was added with the LB medium before film casting). Except for the *r* value, the preparation conditions were identical to previous protocols, and each plate contained the same number of bacterial cells ( $10^6$  cells per plate). Figure 4B shows that there is a low threshold value around *r* = 7, below which the encapsulation procedure leads to complete inactivation. We believe that inactivation by low *r* value precursors is caused by dehydration of the cells (ES2R or RS2R) during the drying period, which leads to faster inactivation of the cells in the dry section of the film. The formation of denser films at low *r* values may also contribute to lower viability though it is not likely to induce the sharp viability threshold that is observed in our studies. The release of methanol may theoretically cause cell inactivation, and it is indeed studied in our laboratory using *E. coli* cells that were genetically modified to report methanol induced stress by increased luminescence. Our preliminary results show that the release of methanol is too slow for complete inactivation of the cells at the corresponding *r* values.

Figure 4C depicts the effect of drying time on the viability of the cells in the silicate matrix. Again, we

used ES2R and RS2R cells induced by MMC and NA, respectively, and the fluorescence intensity 17 h after exposure to the inducer was taken as a measure for the cells' viability. Short drying periods (<4 min) resulted in a mechanically unstable film which was washed out during the rinsing stage. Longer drying periods (> ca. 8–12 min) led to a gradual decrease of the induced luminescence, indicating lower residual cell viability in the dried films. A drying time of 5 min was therefore selected for further studies.

Figure 4D shows the fluorescence dependence on film thickness. We deposited a constant concentration of the precursors on each plate. Thus, the number of cells was linearly dependent on the cell thickness as measured by optical microscopy (we used  $10^6$  cells for the 0.1 mm film), which explains the linear response obtained. The scatter of data for the thick film is probably caused by oxygen limitation which governs the cell response for the thick films.

The encapsulated *E. coli* cells maintained viability for a very long period in the silicate film. To check the viability, we conducted the following test. Several identical biohybrids, containing the same number of cells, were stored at 4 °C for over 3 months and at intervals exposed to the inducer for 17 h. The fluorescence intensities at this time point are depicted in Figure 5 as a function of storage time. The test provides a measure for the ability of the cells to sense the inducer and respond by the expression of the fluorescent protein. This ability is a measure for the viability of the cells.

Figure 5 depicts the viability of E3 *E. coli* cells during prolonged immersion in LB medium. Aside from the proven shelf life stability that can be observed in Figure 5, the reader may notice that the response is rather constant even after long immersion of the cells in the nutrient rich medium. The relative standard deviation of the five data points in Figure 5 is less than 6%. The relative standard deviation of the response of six different samples to the same test conditions 1 day after preparation of the hybrids was also 6%.

This high stability of the response after long storage duration is interesting because *E. coli* cells tend to proliferate very rapidly in nutrient broth (doubling in less than 1 h), and thus one would expect a much larger response after a month of storage if viability and proliferation ability are maintained. Indeed, in nonimmobilized cultures cell proliferation precluded the ability to measure the optical response after 2 days. The

(23) Slonczewski, J. L.; Foster, J. W. pH-regulated genes and survival at extreme pH. In *Escherichia coli and Salmonella Cellular and Molecular Biology*, 2nd ed.; Neidhardt, F. C., Eds.; ASM Press: Washington, DC, 1996; p 1539.

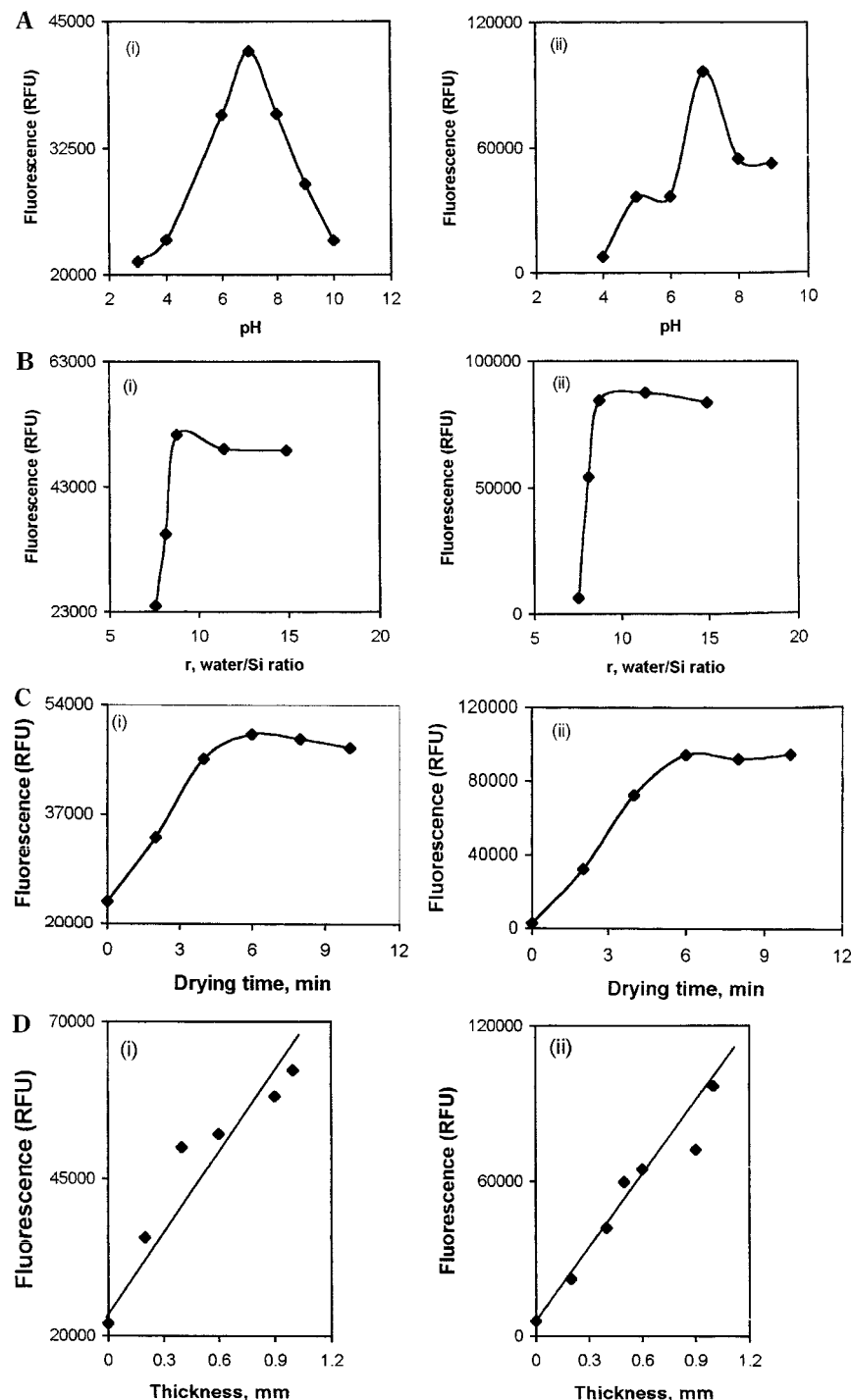


**Figure 4.** Fluorescence response of encapsulated cells for different preparation protocols: (A) Fluorescence response of (i) a ES2R-silicate sensor after exposure to  $1.2 \mu\text{M}$  MMC solution in LB medium and (ii) a RS2R-silicate sensor after exposure to  $0.25 \text{ mM}$  NA solution in LB medium as a function of the sol-gel preparation pH. The silicate films were prepared using LB medium of the specified pH. A 17 h induction time was used.  $10^6$  cells were used for each test. (B) Fluorescence response of (i) ES2R-silicate hybrids as a function of  $r$ , the water/silicon molar ratio after 17 h of induction in  $1.2 \mu\text{M}$  MMC in LB medium, and (ii) RS2R-silicate hybrids as a function of  $r$ , the water/silicon molar ratio after 17 h of induction in  $0.25 \text{ mM}$  NA in LB medium. An identical number of cells ( $10^6$ ) were incorporated in each sensing element. (C) Relative residual viability of (i) ES2R cells and (ii) RS2R cells after drying for the specified amount of time, immediately following the deposition of the silicate precursors on the glass slides. Fluorescence after 17 h of exposure to LB medium containing (i)  $1.2 \mu\text{M}$  MMC and (ii)  $0.25 \text{ mM}$  NA was used as a measure for residual cell viability. Each test was conducted with  $10^6$  cells. (D) Fluorescence response of (i) ES2R-silicate films and (ii) RS2R-silicate films as a function of film thickness after 17 h of induction time in (i)  $1.2 \mu\text{M}$  MMC and (ii)  $0.25 \text{ mM}$  NA in LB medium. A constant concentration of cells was used for film preparation, resulting in a linear dependence of the number of cells on film thickness ( $10^6$  cells/film were used for the preparation of the  $0.1 \text{ mm}$  thick film).

confocal microscopy studies outlined below provide an explanation for the long-term stability of the response.

**Confocal Microscopy Studies.** The fluorescence data that were provided in the previous sections of this

article are based on bulk measurements, and as such they leave many unanswered questions related to the behavior of individual cells in the silicate cages and to their distribution within the silicate films. The use of

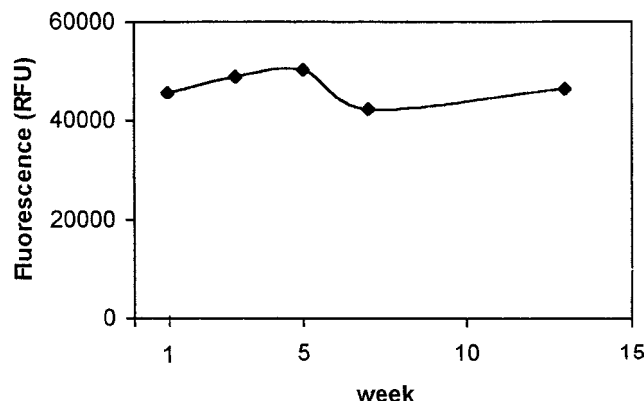


**Figure 5.** Stability studies of a ES2R *E. coli* reporter sensor in silicate. The sensor was prepared with the preparation conditions of Figure 2. The sensors were stored in a refrigerator. In each test, thorough rinsing of the sensing element with LB medium was first used followed by immersion of the sensing elements into LB medium solution containing the inducer (1.2  $\mu$ M MMC). The signal was recorded for 17 h at 25  $^{\circ}$ C.  $10^6$  cells were used for each test.

fluorescent cells allowed use of confocal microscopy, which resolves some of these questions.

**Distribution of the Encapsulated Cells within the Silicate Matrixes.** The bulk fluorescence data that were presented and discussed thus far do not provide a definite description of the location and distribution of the active encapsulated bacteria within the silicate films. Theoretically, it is possible to claim that the cells are strongly attached to the outer layer of the silicate either by physical adsorption or by partial coating with a thin silicate film. Partial coating of cells by vapor-deposited silicate films is indeed a successful encapsulation method that was developed by Carturan and co-workers.<sup>6</sup> It is also possible to claim that the cells are entrapped in cracks and crevices or that they are localized in the interface between the silicate film and the glass slide support. To investigate the depth distribution of the cells within the silicate matrixes, we conducted the following test. Equal numbers of ES2R and RS2R cells were incorporated in the same film (approximately 160  $\mu$ m in thickness), and after induction for 24 h in 1.2  $\mu$ M MMC, the film was studied by confocal microscopy. We took 80 images of 150  $\times$  150  $\mu$ m<sup>2</sup> sections of the film, slicing the film depth at 2  $\mu$ m intervals. Parts A–G of Figure 6 depict several fluorescence images of such virtual slices. The 80 images are available on request. For clarity we also show two sections of the slices at higher magnification (lower two frames in Figure 6, taken from the exact midthickness of the film) that allow visualization of individual fluorescent sites. The red and green colors correspond to reconstruction of the red (583 nm) and green (510 nm) emissions.

Confocal microscopy provides the following unequivocal conclusions: (1) The cells are homogeneously distributed within the silicate film, though their distribution is not uniform and there are areas with different concentrations of cells. The cells are not preferentially distributed in the outer section of the film, and they are not localized in cracks or cervices. (2) The cells are either segregated in very small clusters of a few cells or located in isolated cages that contain a single bacterium per

cage. (3) Active, fluorescent (and thus viable) cells are present even deep inside the film, which shows oxygen availability even at such locations. (4) Dual populations can coexist within the same silicate matrix.

#### Dynamic Studies with a Confocal Microscope.

Figure 5 showed that silicate biohybrids exhibited a constant response even after exceedingly long immersion in LB medium. One of the postulated reasons for such behavior is that encapsulated cells lose their ability to divide because of the physical constraint imposed by the silicate cages. Therefore, even after long immersion in LB medium, the silicate still contains a constant number of cells. It should be noted that this is not the sole possible explanation. It is theoretically possible that oxygen deficiency after long exposure limits the active section in the biohybrid to a thin boundary layer near its top. Since fluorescence is dependent on oxygen availability, a constant fluorescence can be obtained even after cell proliferation. To examine the cells' tendency to proliferate within the silicate matrixes, we conducted single-cell dynamic induction tests. A thick ES2R–silicate biofilm was immersed in LB medium containing 1.2  $\mu$ M MMC and examined periodically with the confocal microscope. Figure 7 shows a set of images that exhibits the evolution of the signal from a specific group of cells (at the middle of the film) as a function of induction time. To evaluate and distinguish the response of caged cells, we have conducted a similar dynamic induction test of ES2R *E. coli* cells that were physically adsorbed on the upper surface of the silicate film. A set of images of the surface of the film showing the increased fluorescence as well as the rapid proliferation of the cells on the film surface is shown in Figure 8. This highlights the difference between cell proliferation on the silicate surface and the stagnation of the number of cells inside the silicate film. Figure 9 shows the results of the last of the confocal microscope studies, the time evolution of the fluorescence intensity and fluorescent area from a specific bacterium as a function of time. The intensity is calculated by integration of the intensity over the fluorescent area. While fluorescence intensity increases gradually (for the arrow-marked cell in Figure 7), the size of the spot remains almost constant, showing that the GFP remains inside or close to the cell and that the cell does not divide. The fluorescent areas of the other cells which were not induced also remained constant. The dimensions of the fluorescent spot corresponded roughly to the dimensions of individual *E. coli* cells (i.e., 1  $\times$  2  $\mu$ m).

On the basis of Figures 7–9, one may reach several conclusions on the viability of cell's in the silicate. However, widely different precursors and pH conditions may lead to different effects of the matrix on a cells' physiology. (1) The cells lose the ability to proliferate within the rigid silicate cages. While the intensity of the GFP fluorescence increases, the area of each fluorescent spot remains constant. (2) The GFP remains either attached to the bacteria or entrapped within the same cavity even after the cell's death. The GFP has a barrel shape of about 2.4 nm<sup>2</sup>. Therefore, its movement within the silicate pores is very limited even after cell death. (3) Figure 7 shows a large variability in cells' responses to induction. While some bacteria are induced and express GFP in response to the specified MMC level,

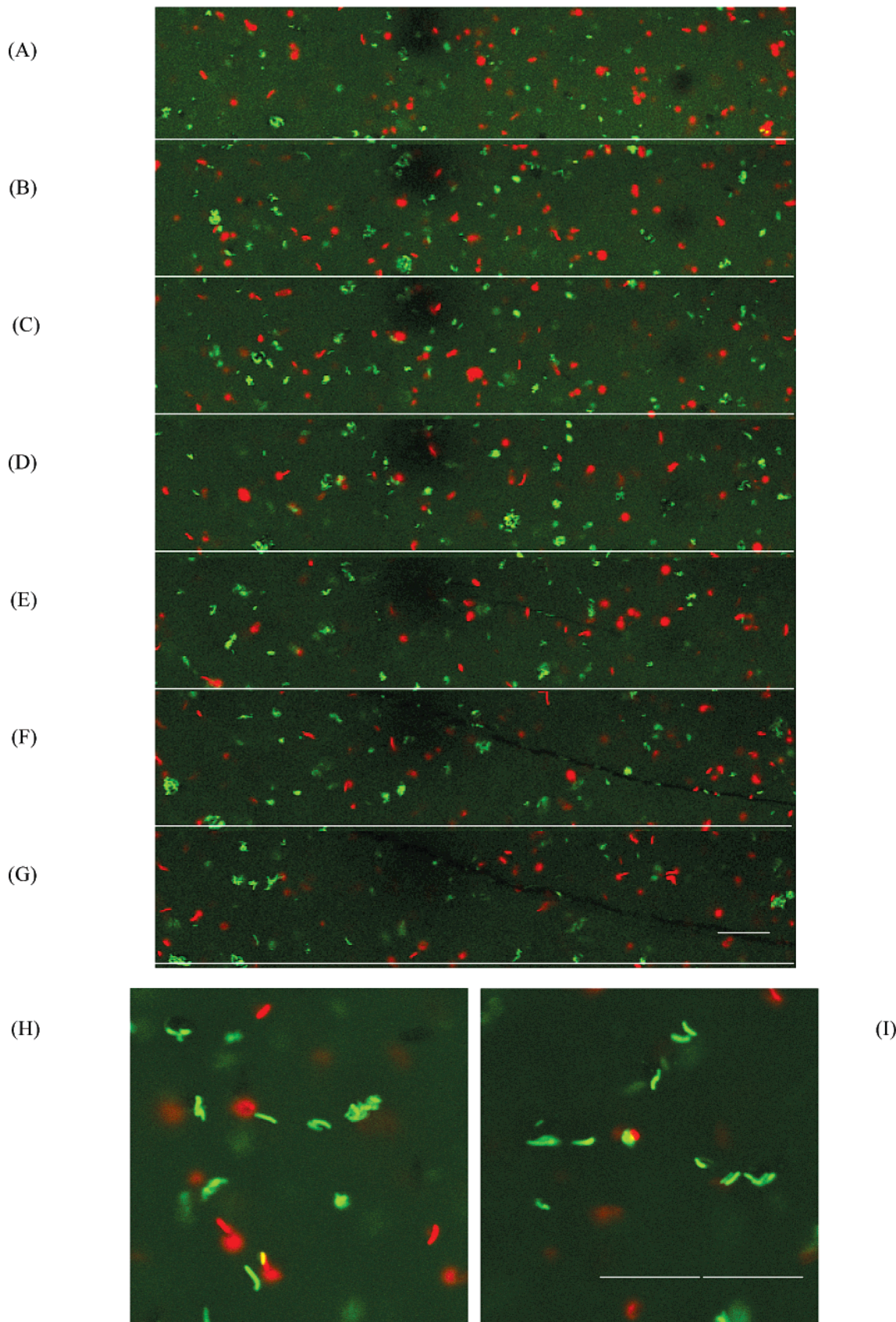


**Figure 6.** Confocal microscopic images of ES2R and RS2R *E. coli* cells in different layers of the silicate matrix, after induction with  $1.2 \mu\text{M}$  MMC, at 17 h. The high-magnification frames were taken at midthickness. The white bar corresponds to  $20 \mu\text{m}$ . Frames A–G correspond to the depths 20, 27, 30, 34, 40, 46, and 51  $\mu\text{m}$ , and frames H and I correspond to 34 and 46  $\mu\text{m}$ .

others either remain inactive (possibly due to cellular damage) or had already produced GFP before the exposure to MMC. (4) Dual bacterial populations can

be sustained within the silicate cages. This is an important conclusion because it is very difficult to maintain stable mixtures of different species in liquid

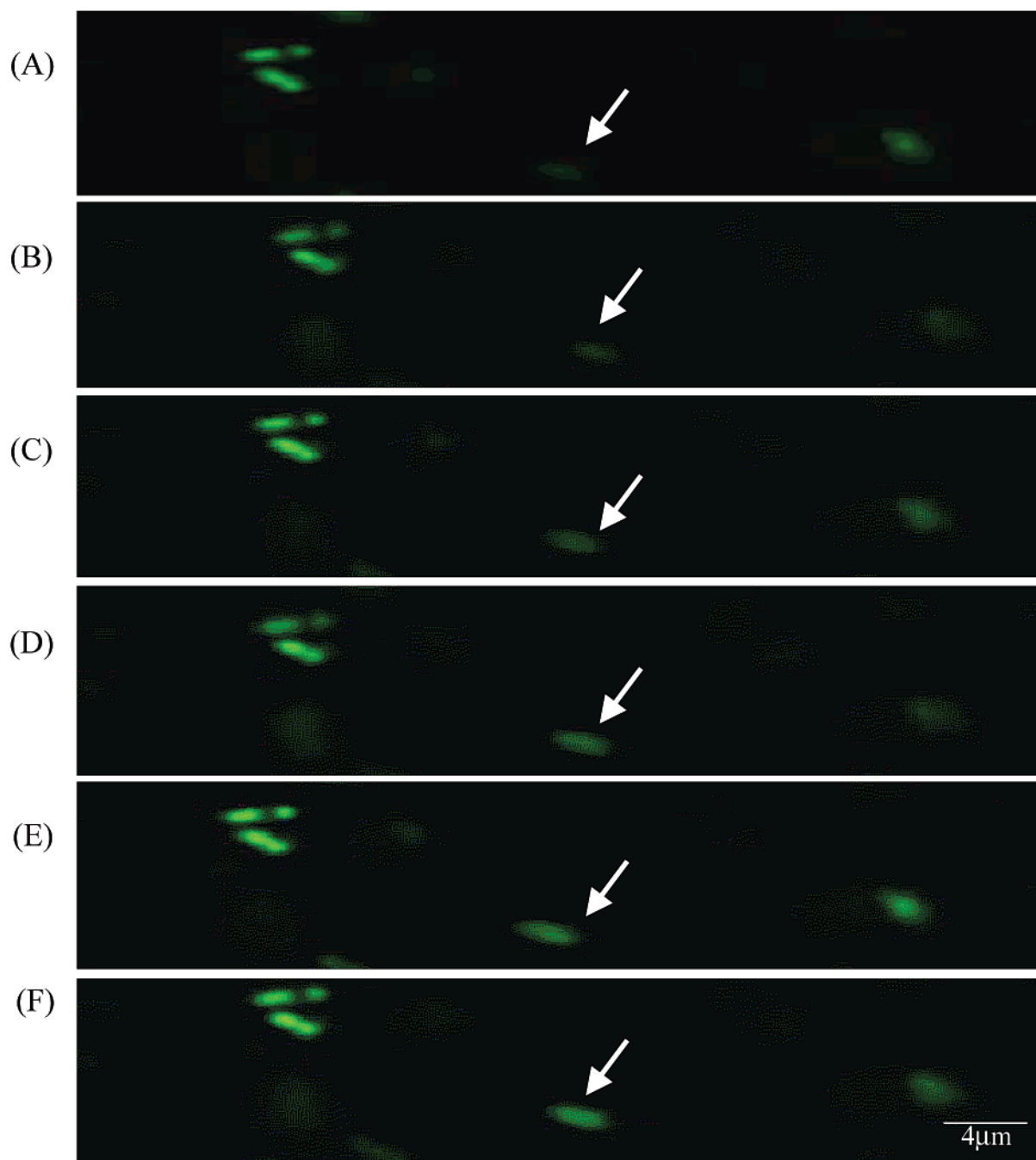


**Figure 7.** Fluorescence intensity study of a single ES2R *E. coli* cell in the sol-gel matrix induced with 1.2  $\mu$ M MMC after different induction times. The incubation times are 0, 140, 260, 340, 420, and 480 min (frames A–F).

culture; in ordinary cell cultures one bacteria strain dominates, usually because of its faster proliferation, ending in a single population. The fact that the bacteria are isolated in segregated cavities implies that dual cultures can be maintained within the same film.

**Special Attributes of the Encapsulated Cells.** The information that was provided in previous sections of this manuscript raises a primary question about the benefits of cell encapsulation. Trivial answers for this question are that encapsulation prevents cells' washout in flow operation, simplifies handling and storage, and endows biocompatibility for in vivo applications. However, several attributes that are illuminated by our studies should be briefly addressed as well. Two practical fields of end applications are kept in mind throughout the following discussion, though in this study we

concentrated on model cells which are not actually meant to fulfill these ends: (1) whole-cell sensing applications—where the cells are used to signal the presence of a compound or set of compounds in the sample; (2) catalytic applications—where the cells are used to destroy or synthesize a specific compound or a set of compounds either in response to a specific signal or on a continuous, unregulated basis.

**Constant Response and Multiple Functionality.** For many sensing applications and particularly those requiring cell exposure to flow conditions or continuous monitoring, practitioners prefer devices that provide a constant response over time. However, unlike chemical reagents, live cells tend to proliferate over time, thus giving enhanced response after long exposure.

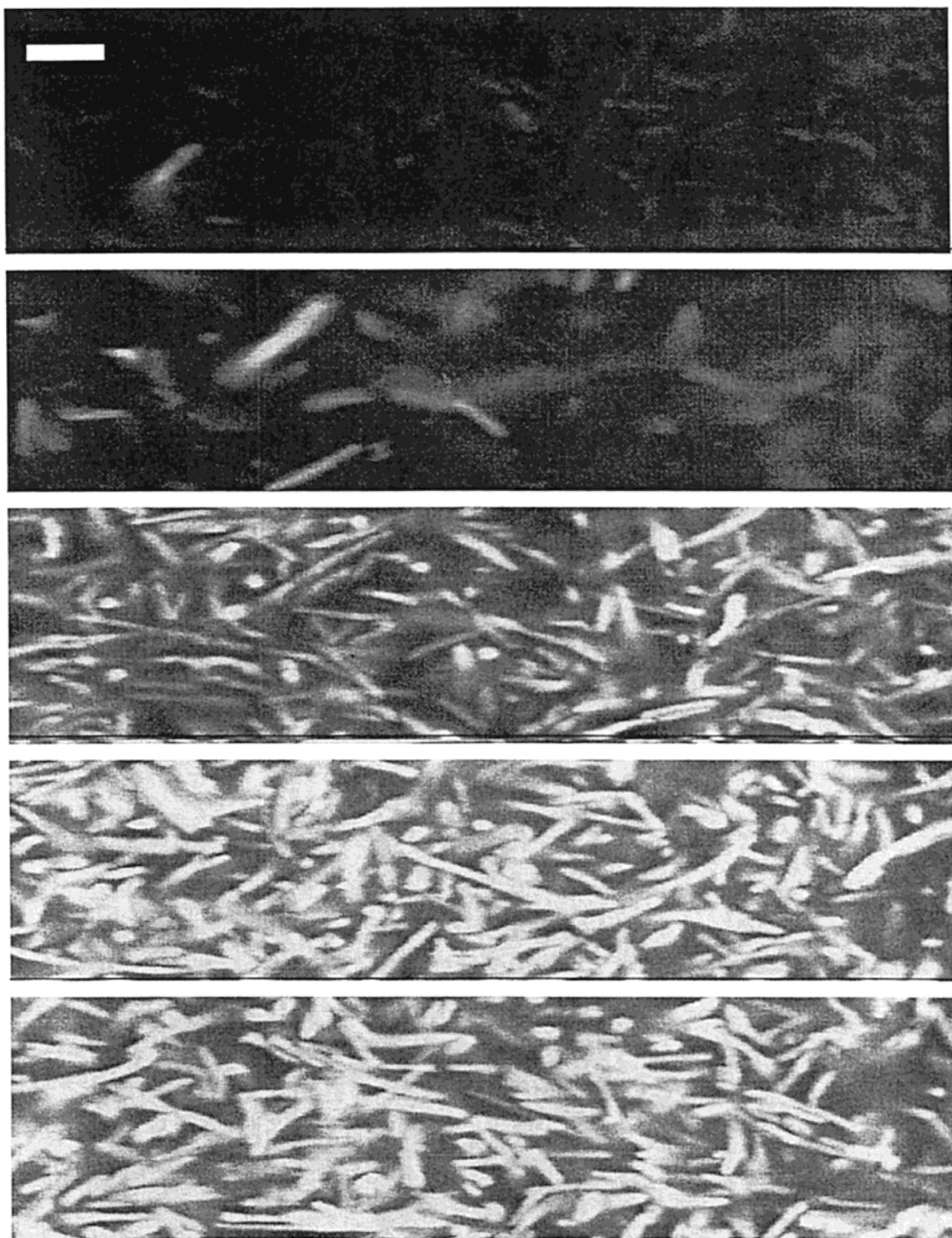


**Figure 8.** Confocal microscopy images of the surface of a silicate film with attached growth of ES2R *E. coli* cells after different induction times by LB medium containing  $1.2 \mu\text{M}$  MMC. The incubation times correspond to 0, 200, 300, 400, and 500 min from top to bottom.

Moreover, for many practical applications one would desire to have a multiple cell culture performing different catalytic or sensing tasks within the same pot. Indeed, sol-gel materials excel in the ability to integrate numerous catalytic and biocatalytic tasks within the same matrix. Recently, Gelman et al.<sup>24</sup> brought this property to its peak by incorporation of acid and base catalysts within the same sol-gel matrix without destroying each other. However, implementation of the

multiple functionality concept to live cells is rather difficult. Usually, a particular strain will adapt better to specific conditions and will take over and dominate the population within the biocatalyst.

Sol-gel encapsulation provides a remedy for these limitations of mixed suspended cultures. The fact that proliferation is prohibited within the silicate network prevents gradual and uncontrolled increase of the response. This constant response can be readily observed in Figure 5, which shows that bacteria that were immersed for a long duration in nutrient broth function as a newly cultivated strain. The complete segregation

(24) Gelman, F.; Blum, J.; Avnir, D. *Angew. Chem., Int. Ed.* **2001**, *40*, 3647.

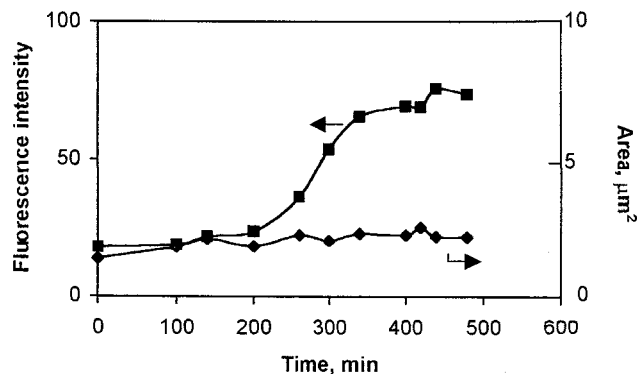


**Figure 9.** Integrated single-cell fluorescence intensity and single domain size as a function of cell induction time. Data are derived from the cell marked in Figure 7.

of the cells to different cellular compartments within the sol–gel matrix, as demonstrated in Figure 6, demonstrates that it is possible to encapsulate different bacteria which excel at different tasks within the same silicate network while maintaining a constant population distribution and preventing dominance of one species. This attribute is of course important for dual sensing by the same sensing element and for multistep synthesis or chemical degradation of organic pollutants by a mixed bacterial population in which each strain specializes in a different reaction step.

**Contamination of the Encapsulated Population and Its Surroundings.** The concern over “leakage” of bacteria and the eventual contamination of our environment by potentially deleterious and resilient bacteria is a serious concern which prevents the widespread use of engineered bacteria in chemical synthesis and environmental cleanup. The use of encapsulated bacteria that do not leach out of the support may in the future form an environmentally acceptable alternative.

To demonstrate this point, we used two differently tagged strains in order to explore whether sol–gel encapsulated bacteria can provide a cure for the contamination of the environment by cell leakage and for

the penetration of the cells from the surroundings to the biohybrid. We immersed a luminous *TV1061 E. coli*–silicate hybrid in a beaker containing concentrated ( $10^8$  cells/mL) ES2R culture and immersed encapsulated ES2R cells in concentrated *TV1061* culture. The cultures contained LB medium to provide nutrients for optimal growth. After several days, we rinsed the biohybrids and investigated leakage of the fluorescent and luminescent bacteria to the respective cultures and the penetration of luminescent or fluorescent bacteria into the hybrid. Luminescence and fluorescence measurements of the four separate phases revealed that the encapsulated cultures were not contaminated by the surrounding cultures, and the bacteria from the hybrids did not leach out of the silicate network.

### Concluding Remarks

Both confocal microscopy and recombinant fluorescence bacteria are powerful tools for the investigation of intact cell–silicate biohybrids. Our investigations of single bacteria fluorescence and the spatiotemporal investigation of the bacteria distribution in the silicate hybrid reveal a few important properties of the biohybrids: The encapsulated cells do not proliferate within the silicate cages. The silicate cages provide a barrier for leaching of the bacteria from the cells and for contamination of the biohybrids by bacteria from the environment. These attributes are important for multitask multiple strain catalysis and sensing.

**Acknowledgment.** This research was supported by the Infrastructure Program of the Ministry of Science and Culture, Israel, by DARPA grant N00173-01-1-6009, and by the Ministry of Science and Culture of the State of Niedersachsen, Germany. Instrumentation was partly funded by the Israel Science Foundation, founded by the Israel Academy of Sciences. We gratefully acknowledge strains provided by T. K. Van Dyk and R. A. LaRossa, the DuPont Company, USA.

CM020020V